AGU PUBLICATIONS

Water Resources Research

RESEARCH ARTICLE
10.1002/2014WR015608

Key Points:
- Soil water availability is expressed as a maximal possible water uptake rate
- It depends on root hydraulic conductance and plant-sensed soil water potential
- The effect of dynamic soil-root radial hydraulic properties is investigated

Correspondence to:
V. Couvreur,
vcouvreur@ucdavis.edu

Citation:
Couvreur, V., J. Vanderborght, X. Draye, and M. Javaux (2014), Dynamic aspects of soil water availability for isohydric plants: Focus on root hydraulic resistances, *Water Resour. Res.*, *50*, 8891–8906, doi:10.1002/2014WR015608.

Received 20 MAR 2014
Accepted 17 OCT 2014
Accepted article online 23 OCT 2014
Published online 18 NOV 2014

Dynamic aspects of soil water availability for isohydric plants: Focus on root hydraulic resistances

V. Couvreur[1,2], J. Vanderborght[3], X. Draye[1], and M. Javaux[1,3]

[1]Earth and Life Institute, Université catholique de Louvain, Louvain-la-Neuve, Belgium, [2]Department of Land, Air and Water Resources, University of California, Davis, California, USA, [3]Institute of Bio- und Geosciences, IBG-3: Agrosphere, Forschungszentrum Juelich GmbH, Juelich, Germany

Abstract Soil water availability for plant transpiration is a key concept in agronomy. The objective of this study is to revisit this concept and discuss how it may be affected by processes locally influencing root hydraulic properties. A physical limitation to soil water availability in terms of maximal flow rate available to plant leaves (Q_{avail}) is defined. It is expressed for isohydric plants, in terms of plant-centered variables and properties (the equivalent soil water potential sensed by the plant, $\psi_{s\ eq}$; the root system equivalent conductance, K_{rs}; and a threshold leaf water potential, $\psi_{leaf\ lim}$). The resulting limitation to plant transpiration is compared to commonly used empirical stress functions. Similarities suggest that the slope of empirical functions might correspond to the ratio of K_{rs} to the plant potential transpiration rate. The sensitivity of Q_{avail} to local changes of root hydraulic conductances in response to soil matric potential is investigated using model simulations. A decrease of radial conductances when the soil dries induces earlier water stress, but allows maintaining higher night plant water potentials and higher Q_{avail} during the last week of a simulated 1 month drought. In opposition, an increase of radial conductances during soil drying provokes an increase of hydraulic redistribution and Q_{avail} at short term. This study offers a first insight on the effect of dynamic local root hydraulic properties on soil water availability. By better understanding complex interactions between hydraulic processes involved in soil-plant hydrodynamics, better prospects on how root hydraulic traits mitigate plant water stress might be achieved.

1. Introduction

1.1. The Concept of Soil Water Availability for Plant Transpiration

As a mere consequence of stomatal opening that is required for photosynthesis, plants transpire considerable amounts of water, which also contributes to nutrient uptake and leaf cooling. Water potential gradients generated by transpiration induce xylem water flow, which propagates via roots to the soil, where a stock of water allows sustaining the transpiration flow. In consequence, the availability of water in soil has a major impact on plant photosynthesis, growth, and yield, which makes it a key concept in agronomy. The definition of soil water availability, first introduced by *Veihmeyer and Hendrickson* [1927] as the amount of water held in the root zone between permanent wilting point (PWP) and field capacity (or soil matric potentials of −15,000 and −300 hPa, respectively), has been broadly discussed over years. In the FAO approach, this quantity is called total available water [*Allen et al*., 1998; *Steduto et al*., 2009]. However, only a fraction of the total available water, which depends on the plant type, transpiration demand, and root development, is readily available. The soil water stress function of *Feddes et al*. [1976] also puts forward that soil water is not equally available in the range between field capacity and PWP, and that an intermediate point of "limited soil water availability" should be considered, below which plant water extraction as well as yield decrease with decreasing soil water potential. In other words, water held by soil matric potentials between the point of limited availability and PWP would still be available, but at a limited rate. In the following years, this model was extended in order to account for experimental evidences that (i) the point of limited water availability depends on plant potential transpiration rate [*Feddes et al*., 1978], and (ii) local reductions of root water uptake (RWU) may be compensated by an increased RWU where water is readily available [*Jarvis*, 1989]. Even though these concepts allow reproducing observed trends qualitatively, they do not rely on a physical representation of hydrodynamics of the soil-plant system [*Javaux et al*., 2013].

In a review paper on soil water availability, *Gardner* [1965] argued that "much of the controversy concerning the relative availability of soil water stems from a failure to define this concept precisely and quantitatively," and stressed that, at that time already, our developing knowledge on processes involved in soil-plant-atmosphere hydrodynamics was making it possible to replace vague concepts by quantitative expressions, which would permit a much better understanding of the relation between soil water potential and water uptake by plants. Doing so, *Gardner and Ehlig* [1963] took distance from the soil-centered point of view on soil water availability, stating that it is a function of both plant and soil hydraulic properties. Using the physical concept of free-energy-driven water flow (i.e., water flows from high toward low water potential regions, at a rate proportional to the water potential difference between both regions, and inversely proportional to the hydraulic resistance of the pathway), they defined plant and soil equivalent hydraulic resistances, which both limit the water flow rate between soil and leaves.

1.2. Identifying Soil and Plant Equivalent Hydraulic Properties

When roots take up water, the three-dimensional (3-D) water flow field in the soil depends on both distributions of RWU and soil hydraulic conductivities, both being functions of the soil matric potential distribution. In order to identify a single soil hydraulic resistance representative for the flow paths in the soil at a given depth, *Gardner and Ehlig* [1963] and more recently *Sinclair* [2005], *Siqueira et al*. [2008], and *Caldeira et al*. [2014] needed to assume that (i) roots are distributed homogeneously at a certain depth, so that all flow paths to the roots have the same length scale and associated flow resistance, (ii) RWU rate is constant, even though the solution is then used in transient conditions, and (iii) soil hydraulic conductivity is an exponential function of soil matric potential. Numerical computation of the matrix flux potential allowed relaxing the third assumption [*De Jong Van Lier et al*., 2006], but the appropriateness of remaining assumptions should however be carefully considered regarding actual system properties [*Couvreur et al*., 2014]. Nowadays, a robust alternative to model the detailed soil hydrodynamics within the root zone is to numerically solve Richards equation in 3-D and couple it to a root water uptake model [*Somma et al*., 1998; *Doussan et al*., 2006; *Javaux et al*., 2008], its drawback being the possibly high computing requirements of the method, in particular when high spatial resolution is requested [*Schroeder et al*., 2009].

Pathways of water from soil-root interfaces to xylem vessels at the plant collar take place in the 3-D network of root hydraulic resistances. Apart from few studies [*Janott et al*., 2011], roots water capacity is generally neglected when modeling crop hydrodynamics (i.e., roots are considered neither to store nor release water, so that the incoming flux equals the outgoing one) [*Doussan et al*., 1998a]. This property allowed *Couvreur et al*. [2012] demonstrating that any network of root hydraulic resistances can be summarized as a single equivalent root system hydraulic resistance, while spatially heterogeneous soil-root interface water potentials can be summarized as a single equivalent soil water potential "sensed by the plant," both fitting in the *Gardner and Ehlig* [1963] approach.

1.3. Time Variable Hydraulic Resistances on the Radial Pathway From Soil-Root Interface to Root Xylem Vessels

Although the equivalent hydraulic resistance of a maize root system was numerically demonstrated to be rather sensitive to the resistance of the radial pathway from soil-root interfaces to root xylem [*Couvreur et al*., 2012], it is still unclear how local fluctuations of these hydraulic resistances would impact the equivalent resistance of the whole root system, and thus soil water availability for the plant.

In the past, plant cell hydraulic properties were considered to be relatively invariant, depending mainly on the permeability of cell membrane lipid bilayer. But since the first plant aquaporin (AQP) was discovered, more than 20 years ago [*Maurel et al*., 1993], a complete shift in the understanding of plant water relations has occurred [*Maurel and Chrispeels*, 2001]. The exclusive flow of water through this selective membrane protein, which can rapidly and reversibly close itself [*Tyerman et al*., 2002; *Chaumont et al*., 2005], extends the potential for control over water flow by living cells. The regulation of AQPs was even shown to radically impact root radial hydraulic conductance, due to the presence of an impermeable layer of cell walls ("Casparian band") on the pathway between soil and root xylem, forcing water to cross cell membranes, and thus AQPs [*Barrowclough et al*., 2000]. With decreasing soil matric potential (negative by definition), abscisic acid (ABA) concentration increases in roots [*Dodd et al*., 2010], which would provoke an increase of AQP activity (i.e., their ability to facilitate water flow through biological membranes), and consequently of

effective root radial hydraulic conductance, at both the cell and the organ level in dry conditions [*Hose et al*., 2000; *McElrone et al*., 2007].

A second type of process potentially impacting soil-root hydraulics is the formation of air gaps at soil-root interfaces, due to the shrinkage of roots and/or soil with decreasing soil matric potential [*Carminati et al*., 2009]. Such gaps reduce the contact area between soil and roots and induce a strong increase of the hydraulic resistance to radial water flow between them. Additional processes are expected to increase the hydraulic resistance between soil and roots, such as the change of root mucilage property toward hydrophobicity in drying conditions [*Carminati and Vetterlein*, 2013]. This particular process occurs upstream of the soil-root interface, but could, for instance, be included in an "extended radial hydraulic conductance" accounting for the rhizosphere properties. Even though the magnitude and dynamics of these processes are not clearly understood today, they most likely impact the hydraulic resistance to radial flow from soil to root xylem more rapidly than root anatomical changes.

Whatever the underlying processes (AQP, gaps, rhizosphere property evolution, . . .), soil drying thus possibly has two opposite consequences on soil-plant hydraulics: either a local increase or a decrease of the radial hydraulic conductance from the soil-root interface to root xylem vessels. How such spatiotemporal variability of soil-root hydraulic properties may affect soil water availability for plant transpiration is however unclear.

1.4. Objectives

This study has two main objectives. The first one is to revisit the classic concept of soil water availability in the light of hydraulic concepts, mainly focusing on the effect of the whole root system hydraulic conductance and soil water potential (SWP) on soil water availability for isohydric plants (i.e., plants whose leaf water potential stabilizes at a critical value during water stress [*Tardieu and Davies*, 1992]). It is addressed in the theoretical background (section 2), using a theoretical inspection of relationships between root water uptake, soil water potential, and root hydraulic parameters, which have been deduced in other studies.

The second objective is to understand how local variations of soil-root radial hydraulic conductances due to variations in soil matric potentials influence soil water availability for plant transpiration. This requires simulating water dynamics in 3-D in the soil, at soil-root interfaces having dynamic hydraulic properties, and inside the root system of a plant (in this case a maize plant), offering an unprecedented insight into the impact of local soil-root processes on water availability for the plant (see sections 3 and 4).

Since we focus in this study on the availability of soil water for plants and on the novel insight in dynamic root hydraulic properties, we allocate the computational effort to the detailed modeling of the significant hydraulic resistances and water potential gradients that occur in the latter compartments (soil and roots). Leaf stomatal regulation is implicitly accounted for through isohydricity, but the details of hydraulic and hormonal signaling that lead to isohydricity are not modeled. Other processes such as carbon fixation and growth interact at long term with soil water availability for plants, but are not in the scope of this study.

2. Theoretical Background

2.1. Limits to Soil Water Availability for Plant Transpiration

Soil water availability for plant transpiration is commonly considered to have the dimension of a volume of water per horizontal soil surface area, expressed as a height of water h_{avail} (L), typically in millimeter units [*Allen et al*., 1998]. This variable represents the total stock of water present in the root zone that the plant is able to transpire, regardless of the time that it would take to do so.

The goal of plant water stress functions (i.e., reduction of transpiration due to water deficit) is to account for the fact that soil water status may limit plant transpiration rate at a certain time, i.e., the rate at which the plant can "consume" soil water. Therefore, the stock h_{avail} is not the only limit to soil water availability for the plant. A general definition of soil water availability for plants should account for both types of limits, by quantifying the stock of water (h_{avail}) and the maximum rate at which water can be supplied by the soil-plant system to plant leaves for transpiration [*Javaux et al*., 2013].

As stated in section 1.2, the instantaneous water flow rate reaching plant leaves depends on the distribution of hydraulic resistances and water potentials between soil-root interfaces and leaves, and increases with decreasing leaf water potential (ψ_{leaf}, P) for a given SWP distribution. When leaves of isohydric plants experience a low critical water potential $\psi_{leaf\ lim}$ (P), a partial closure of stomata prevents their water potential from dropping further by reducing transpiration rate [*Tardieu and Simonneau*, 1998]. Even though isohydricity has been observed for decades [*Tardieu and Davies*, 1992; *Loewenstein and Pallardy*, 1998; *Fisher et al*., 2006; *McDowell et al*., 2008], the mechanisms that provoke the emergence of isohydricity are not well understood yet, but would involve a control of stomatal conductance by ψ_{leaf} and ABA concentration [*Tardieu and Simonneau*, 1998; *Tuzet et al*., 2003; *Christmann et al*., 2007; *Franks et al*., 2007; *McAdam and Brodribb*, 2014; *Huber et al*., 2014]. An example of benefit of such a regulation is the prevention of cavitation [*Cochard et al*., 2002]. During isohydric water stress, water flow rates cannot increase by further decreasing ψ_{leaf}. The water flow rate toward leaves at $\psi_{leaf\ lim}$ is thus the maximum flow rate the plant can obtain (for a given combination of SWPs and plant hydraulic resistances) and will be called the available water flow rate for plant transpiration: Q_{avail} ($L^3\ T^{-1}$).

Definitions of water availability in terms of a flow rate already exists in other domains: for instance, for pumps [*Jennings*, 1996], river flow [*Sene et al*., 1999], or dams [*Gracheva et al*., 2009]. Such a concept can also be compared to the principle of "offer and demand." Q_{avail} is equivalent to the "offer of water" from the soil-root system while the plant potential transpiration rate (T_{pot}, $L^3\ T^{-1}$) is the "demand for water" defined in nonwater-limiting conditions by atmospheric conditions and leaf properties. When the offer of water is higher than the demand, the actual plant transpiration rate (T_{act}, $L^3\ T^{-1}$) equals T_{pot} (and $\psi_{leaf} > \psi_{leaf\ lim}$). Otherwise ($T_{pot} > Q_{avail}$), the plant being assumed not to have a water capacitance, water outflow does not exceed the inflow. Hence, T_{act} equals Q_{avail} (and $\psi_{leaf} = \psi_{leaf\ lim}$ by definition). In the latter case, the plant is considered to experience a period of water stress.

This can be summarized as:

$$T_{act} = min\left(T_{pot}, Q_{avail}\right) \tag{1}$$

Note that the definition of isohydric water stress and prescribed T_{pot} implicitly assume that leaf stomatal conductance is not affected by plant water status when $\psi_{leaf} > \psi_{leaf\ lim}$ [*Damour et al*., 2010] and becomes null for $\psi_{leaf} < \psi_{leaf\ lim}$. In addition, keeping $\psi_{leaf} = \psi_{leaf\ lim}$ under water stress is a constraint sufficient to identify a single possible value of T_{act} given the soil-plant system state and properties. In consequence, a detailed stomatal conductance model is not necessary to determine plant transpiration rate in this study, but it would be necessary in case the considered plant would not be isohydric or if T_{pot} was not prescribed, as in *Tardieu and Simonneau* [1998].

2.2. Bridging a Gap Between Empirical and Mechanistic Water Stress Functions

The water flow available to plant leaves can be related to plant-scale hydraulic properties, using the model of *Couvreur et al*. [2012], which relies on the same representation of water flow in HA as RSWMS [*Javaux et al*., 2008] to predict plant collar water potential (ψ_{collar}, P):

$$\psi_{collar} = \psi_{s\ eq} - \frac{T_{act}}{K_{rs}} \tag{2}$$

where K_{rs} ($L^3\ P^{-1}\ T^{-1}$) is the root system hydraulic conductance, and $\psi_{s\ eq}$ (P) is the equivalent SWP "sensed by the plant" (i.e., a plant HA sensitive SWP):

$$\psi_{s\ eq} = \sum_{j=1}^{N} \psi_{sr,j} \cdot SUF_j \tag{3}$$

where SUF_j (-) is the root system Standard Uptake Fraction at the jth soil-root interface (which corresponds to the fraction of RWU allocated to the jth soil-root interface under uniform SWP conditions; note that the sum of SUFs is 1 by definition), $\psi_{sr,j}$ (P) is the SWP at the jth soil-root interface, and the j index ranges from the first to the last of the N root segments. It should be noted that the water potentials defined above include gravitational and matric water potentials, and could include the osmotic potential as in *Schröder et al*. [2014]. It is further worth noting that, by measuring predawn plant water potential, several authors,

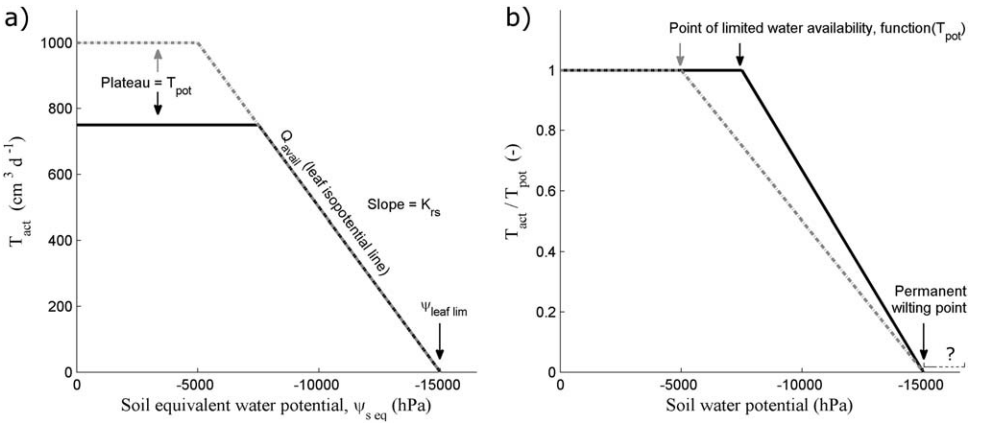

Figure 1. (a) Example of actual transpiration rate reduction predicted by the mechanistic model with high (dashed gray line) and low (solid black line) potential transpiration rates. (b) Classic plant water stress function with the ratio of actual to potential transpiration rate used as ordinate. The coincidence between the permanent wilting point and intercept of the empirical water stress function is stressed not to be clear.

among whom *Kolb and Sperry* [1999], actually measured $\psi_{s\ eq}$ (when T_{act} is null, $\psi_{leaf}=\psi_{collar}=\psi_{s\ eq}$, see equation (2)).

In the following, ψ_{leaf} is assimilated to ψ_{collar} as for crops the resistance to water flow from plant collar to leaves is considered as negligible as compared to the root system hydraulic resistance [*Frensch and Steudle*, 1989]. This assumption could however be easily relaxed by including the collar-to-leaves hydraulic resistance in K_{rs} in order to directly predict ψ_{leaf}. Under water stress, equation (2) determines the following form of the water flow rate available to the leaves of an isohydric plant:

$$Q_{avail}=K_{rs}.\left(\psi_{s\ eq}-\psi_{leaf\ lim}\right) \tag{4}$$

Combining equations (1) and (4) yields:

$$T_{act}=min\left[T_{pot},K_{rs}.\left(\psi_{s\ eq}-\psi_{leaf\ lim}\right)\right] \tag{5}$$

Since T_{pot} is independent of $\psi_{s\ eq}$, and Q_{avail} is a linear function of $\psi_{s\ eq}$, T_{act} is a piecewise linear function of $\psi_{s\ eq}$ with a plateau at high values of $\psi_{s\ eq}$ (see Figure 1a). Three characteristic values determine the shape of this function: (i) $\psi_{leaf\ lim}$ is the intercept of the function on the abscissa axis, (ii) K_{rs} is the slope of the function, and (iii) T_{pot} is the height of the plateau.

Note that the Q_{avail} limit is a leaf water "isopotential" line. In other words, the leaf water potential is the same all along this straight line (and equals $\psi_{leaf\ lim}$). In Figure 1a, a decrease of $\psi_{leaf\ lim}$ to −16,000 hPa, would result in a 1000 hPa rightward translation of the Q_{avail} limit, which would then be located on the "−16000 hPa leaf isopotential line."

This mechanistic isohydric water stress function shares similarities with plant transpiration reduction functions characterized empirically for different crops by numerous authors, among whom *Gardner and Ehlig* [1963], *Tanner* [1967], *Wesseling* [1991], and recently *Schoppach and Sadok* [2012]. These authors observed the relative plant transpiration (ratio of plant actual transpiration rate T_{act} to the transpiration rate of a control plant in a well-watered conditions T_{pot}), to drop rather linearly, either as a function of soil water content or of SWP, and to reach zero at a point higher or equal to the PWP (assigned to be −15,000 hPa in the soil physics community), see typical shape in Figure 1b.

Three main differences can be noted between the mechanistic water stress function in Figure 1a and the typical empirical function in Figure 1b. First, empirical functions generally use the ratio T_{act}/T_{pot} as ordinate, instead of T_{act}. In such condition, the slope of the mechanistic water stress function would become K_{rs}/T_{pot}, and thus, change with plant potential transpiration, which is indeed a property of empirical water stress functions [*Feddes et al.*, 1978; *Wesseling*, 1991; *Novak and Havrila*, 2006]. It is however not clear if the slope of empirical water stress functions would become unique if their ordinate axis was T_{act}. Second, empirical water stress functions generally use the SWP (or soil water content) as abscissa, instead of the plant-sensed

SWP ($\psi_{s\ eq}$). Depending on where the SWP is measured (depth, proximity to roots, etc.), it might be well correlated with but not necessarily equal to $\psi_{s\ eq}$. Note that in conditions of dense rooting, like for plants grown in small pots, the SWP is generally considered as uniform and may be considered equal to $\psi_{s\ eq}$. Third, even though the intercept of empirical water stress functions corresponds to the SWP at which soil water is not available to the plant anymore, it is not given that it coincides with the PWP and $\psi_{leaf\ lim}$. Especially, PWP tends to be considered as a universal soil property while $\psi_{leaf\ lim}$ is a plant property depending on stomatal regulation, and thus may be species and even genotype dependent [*Gardner and Nieman*, 1964]. Differences between these properties might arise from the way SWP is measured too. Observations of the plant-sensed SWP, for instance, by measuring ψ_{leaf} when the plant stops transpiring (then $\psi_{s\ eq}=\psi_{leaf}$), would provide elements of a response.

In the conceivable case, these three main differences were insignificant, existing empirical water stress functions would deliver values of K_{rs} and $\psi_{leaf\ lim}$, while measurements of K_{rs} and $\psi_{leaf\ lim}$ would represent a convenient way to shape our future empirical plant water stress functions.

3. Methodology

The second objective (i.e., understanding how local variations of soil-root radial hydraulic conductances due to variations in soil matric potentials influence soil water availability) requires the use of the modeling platform R-SWMS [*Javaux et al*., 2008] to run simulations explicitly accounting for the three-dimensional water flow in the soil, at soil-root interfaces, and inside the root system hydraulic architecture (HA). Different functions of relative root radial conductance to soil matric potential are considered. For each of them, the evolution of plant actual transpiration T_{act}, plant collar water potential ψ_{collar} (considered as a proxy of leaf water potential ψ_{leaf}), equivalent SWP sensed by the plant $\psi_{s\ eq}$, and root system hydraulic properties, are examined during a 1 month drought scenario.

Scenario features and system properties are described in more details in the following subsections.

3.1. Root System Properties

An 80 days old maize root system of 35,000 root segments generated with *RootTyp* [*Pages et al*., 2004] and described in detail by *Couvreur et al*. [2012] is used for all simulations. Its architecture is based on *Girardin* [1970], *Tardieu* [1988], and *Tardieu and Pellerin* [1990].

Default maize root hydraulic properties, sensitive to root segment age and type (see Figures 2a and 2b, respectively, for principal and lateral roots), were obtained from *Doussan et al*. [1998b] and *Girardin* [1970]. At the whole root system level, they constitute the "default" HA.

A multiplicative factor of basic root radial hydraulic conductance is used to represent the sensitivity of root radial conductance to soil matric potential. The multiplicative factor is a function of the current soil matric potential only. Consequently, no hysteresis effect is accounted for. Yet, different functions are used for different types of sensitivity to soil matric potential (see Figure 2c).

A first function, referred to as "Gap" (in red in Figure 2c), decreasing linearly with decreasing soil matric potential is assumed to represent (in a simplified way) the consequence of processes such as the formation of air gaps or of a hydrophobic layer at soil-root interfaces. The start of the decrease occurs at a matric potential of −500 hPa, at which *Carminati and Vetterlein* [2013] observed the formation of air gaps around lupin roots, and the function reaches zero relative hydraulic conductance at −15,000 hPa, at which a complete detachment of roots from the soil is assumed. We are aware that a detailed modeling of root shrinkage or rhizosphere hydrophobicity would demand a considerable increase of the model complexity. The poor quantitative understanding of these processes however justifies the current use of rather simple representations.

The second function, referred to as "AQP" (in blue in Figure 2c), represents processes expected to locally increase radial conductivity with decreasing soil matric potential, for instance, a regulation of AQP activity. According to measurements of ABA concentration effect on root radial conductivity [*Hose et al*., 2000] and to measurements of soil matric potential effect on ABA concentration in roots [*Dodd et al*., 2010], in the range of soil matric potentials from −50 to −1000 hPa, root radial conductance would be subject to a

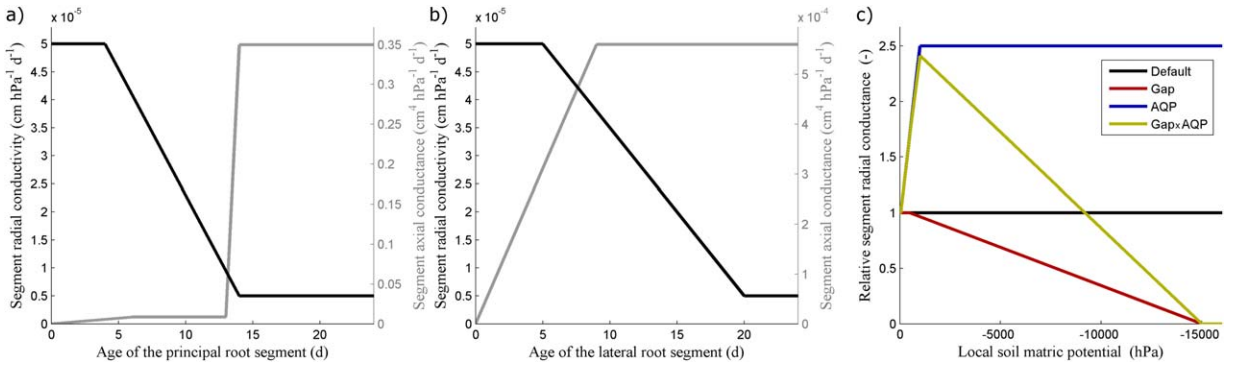

Figure 2. Detailed root segment hydraulic properties description: axial and radial conductivities related to root segment age for (a) principal and (b) lateral roots. (c) Multiplying factors of roots radial conductances, related to local soil matric potential (reaction to soil matric potential considered as instantaneous and reversible). These factors could, respectively, be interpreted as the result of the formation of air gaps at soil-root interfaces (red), an increased aquaporin activity (blue), and both types of processes (yellow).

relative increase of 250%. Due to the lack of data available in the literature, the relative radial conductance is considered to reach a plateau at lower (more negative) soil matric potentials.

A third intermediate function, product of the first two ones, and referred to as "Gap x AQP" (in yellow in Figure 2c), is also used in order to combine the trends of both of the first two functions.

It must be noted that AQP activity and root shrinkage might also be considered to be a function of the root xylem water potential, which would lead to enhanced fluctuations of radial conductances. The choice of the soil matric potential as the independent variable of the relative radial conductance is based on the fact that the quantitative information currently available in the literature only links these two variables (sometimes indirectly). In case future research demonstrates that other variables (e.g., water potential in stele or cortex cells) are main variables that determine changes in radial conductance, a more detailed modeling of the radial pathways from soil to root xylem might be necessary.

Note that no root growth and no change in root ages are considered during the simulations, so as to focus on the effect of the studied local processes on dynamic plant hydraulics. Yet, although the different plants have the same constant root architecture, only the default HA remains constant. "Gap," "AQP," and "Gap x AQP" HAs evolve differently in time, due to the different sensitivity of their hydraulic properties to soil matric potential, and to diverging soil matric potential distributions of their respective simulations.

The macroscopic hydraulic parameters K_{rs} and **SUF** presented in section 2.2 are characterized at each time step with updated root segments hydraulic properties, using the method proposed by *Couvreur et al.* [2012]. In section 4.2, they are used as interpretation key of the water uptake dynamics simulated with R-SWMS. The **SUF** also allows calculating the plant-sensed SWP.

3.2. Scenario Description

The chosen scenario represents a summer drought of 31 days, with a daily transpiration rate (T_{daily}, $L^3\ T^{-1}$) of 600 $cm^3\ d^{-1}$ (i.e., 5.3 mm d^{-1} for an average of approximately 9 plants m^{-2}). Sinusoidal daily variations of T_{pot} (implicitly accounting for atmospheric conditions and leaf properties in nonwater-limiting conditions) are applied as "flux-type" boundary condition of the soil-plant system, so that the instantaneous potential transpiration rates range from zero at midnight to 1200 $cm^3\ d^{-1}$ at noon. Water potential heterogeneity between leaves is neglected as they are connected by highly conductive xylem vessels, which is in agreement with the fact that maize leaves react simultaneously to water deficit [*Chenu et al.*, 2008]. For the same reason, ψ_{collar} is used as proxy of ψ_{leaf}. This assumption might however be inappropriate for certain types of plants [*Domec and Pruyn*, 2008]. At each time step, ψ_{collar} is calculated by solving 3-D soil water flow as well as root segment-scale water flow equations from soil-root interfaces to plant collar. When reaching the value $\psi_{leaf\ lim}$ (set at −15,000 hPa), the boundary condition switches to "potential type" in order to simulate isohydricity. The actual transpiration rate (T_{act}) is then calculated from water flow equations so as to respect the constant $\psi_{leaf\ lim}$. Isohydricity is thus assumed as emergent behavior, thereby avoiding the modeling of the complex mechanisms of stomatal regulation that lead to isohydricity.

In order to represent the overlapping of different maize root systems, as it would occur in a field, while limiting the computational needs, the generated root system was located in a periodic soil domain of 15 cm (direction of the maize rows) on 75 cm (direction perpendicular to the maize rows). This domain was periodic at its vertical boundaries for soil water fluxes, root system architecture and root water fluxes. The soil spatial discretization (in all directions) was 1.5 cm. No-flux boundary conditions were set at top and bottom boundaries of the soil domain, so as to focus on the influence of plant water uptake on soil water availability.

A soil with high water capacity and hydraulic conductivity for a wide range of soil matric potentials was chosen so that soil water availability gradually decreased during the simulated period. A silt loam parameterization [*Carsel and Parrish*, 1988] of Mualem-Van Genuchten equations [*Van Genuchten*, 1980] was therefore selected. Initially, the SWP at the top of the soil profile is set to field capacity (−300 hPa), and the 123 cm deep soil profile is at hydrostatic equilibrium with the top. Note that the osmotic potential is neglected in this study.

4. Results and Discussion

In further subsections, we investigate how relations between root segment radial conductances and soil matric potential (see sections 1.3 and 3.1) would affect: (i) the dynamics of plant water status variables, (ii) the macroscopic plant hydraulic properties, and (iii) the Q_{avail}.

4.1. Dynamics of Plant Actual Transpiration and Water Potential

Figure 3a shows the evolution of T_{act} for each scenario. Q_{avail} becomes progressively limiting (i.e., lower than T_{pot}) for each HA: first for "Gap" (day 12), then "Default" (day 13), "Gap x AQP" (day 17), and finally "AQP" (day 18). This ranking is expected based on the evolution of root segments' radial conductances in drying conditions (see Figure 2c) resulting in delayed water stress for HAs with higher radial conductances.

Even though they were the first to experience water stress, after day 26 "Default" and "Gap" were transpiring slightly more (on a daily basis) than, respectively, "AQP" and "Gap x AQP." An explanation for this changing trend is that the environment of the latter group was much drier after day 26, due to their delayed reduction of transpiration rate. These behaviors could be considered as two possible opposite strategies of plants during drying phases: the former group reducing their access to water and hence transpiration rates earlier in order to save water for future needs, while the latter group would access water with the highest competitiveness. This point illustrates that even though possible mechanisms increasing root hydraulic conductance in conditions of drought temporarily increase soil water availability (through Q_{avail}), when it comes to questions of long-term management of a limited water resource, the timing of soil water availability also matters [*Lobet et al*., 2014]. For instance, it was experimentally demonstrated that in environments subject to long dry spells, promising root traits to be selected for drought tolerance actually limit the access to water in the early season [*Kholova et al*., 2010] in order to keep it available for critical stages of crop growth, during which a water deficit can have dramatic consequences on yield [*Khodarahmpour and Hamidi*, 2012].

Root hydraulic redistribution, i.e., water flow from wet to dry regions of the soil profile through the root system [*Dawson*, 1996; *Caldwell and Richards*, 1989], is thought to improve soil water availability by refilling drier regions with water, mostly overnight. This process naturally occurred in the simulations due to the connected nature of soil and root HAs. During the last 4 days, the "Default" HA transpired 200 $cm^3\ d^{-1}$ on average while 41 cm^3 were lifted to dry regions daily, thus contributing to approximately 20% of the daily uptake. On the opposite, only 11% of water availability was sustained by hydraulic redistribution for the "Gap" HA whose roots were hydraulically disconnected from dry soil. Eventually, respectively, 26 and 15% of the "AQP" and "Gap x AQP" HAs' water availability relied on hydraulic redistribution during the last 4 days of the drought. These ratios are of the same order of magnitude as reported by *Caldwell and Richards* [1989] and *Brooksbank et al*. [2011] (respectively, 34 % and 27% for Sage Brush and Eucalyptus), and can be expected to be significantly sensitive to processes altering soil-root xylem conductivity.

Figure 3b shows the evolution of ψ_{collar} (considered as a proxy for ψ_{leaf}) for each scenario. Due to the drought, the general trend of ψ_{collar} is decreasing. The impact of the day-night cycle of plant transpiration is also very clear, with minima of ψ_{collar} around noon and maxima at night, as typically observed experimentally [*Gardner and Nieman*, 1964; *Shackel*, 2011]. During the last 2 weeks of the simulation, ψ_{collar} of "Gap"

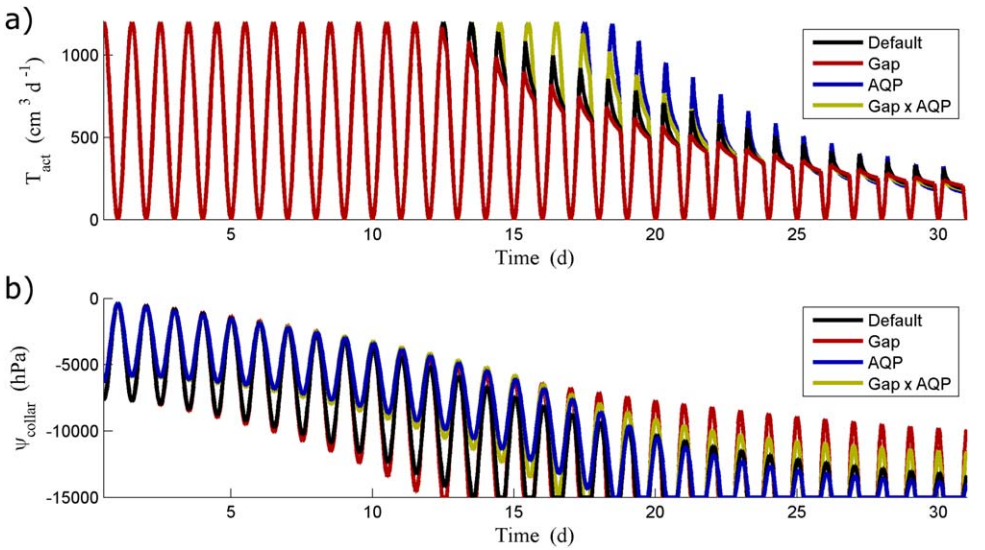

Figure 3. Evolution of (a) plant actual transpiration rate and (b) plant collar water potential during the 1 month drought scenario, for the four types of hydraulic architectures.

and "Gap x AQP" HAs recovered to significantly higher values at night. Note that ψ_{collar} never reached values lower than −15,000 hPa due to the assumed isohydric regulation of T_{act} by stomata.

The relation between the cumulative amount of water transpired and the equivalent SWP sensed by each HA ($\psi_{s\ eq}$, a spatially averaged soil-root interface water potential) is shown in Figure 4a. For a given cumulative transpired water, "Gap" roots always preserved a higher and less fluctuating $\psi_{s\ eq}$, partly explained by the fact that it took up water at a slower rate, thus limiting water depletion around roots. However, even though the "Gap x AQP" transpired at a higher rate and did less hydraulic redistribution than the "Default" HA, it preserved higher $\psi_{s\ eq}$ and ψ_{collar}. Additional explanations are thus necessary, such as changes in the way RWU was distributed for each HA (for instance, due to changes in the **SUF**), which will be discussed in the next subsection.

It is worth noting that the impact of plant growth, was not considered in these simulations, and might have led to different results regarding the access to water. For instance, the "AQP" HA, which transpired more, might have formed more photosynthesis products, grown deeper roots, and consequently increased its Q_{avail}.

4.2. Dynamics of Macroscopic Hydraulic Parameters

In this section, the macroscopic hydraulic model presented in equations (2) and (3) is used as interpretation key of the results simulated with R-SWMS. Summarizing the collection of locally dynamic root hydraulic properties as evolving macroscopic parameters helps interpreting the results of the previous section.

Even though the root system architecture remains constant in simulations presented in this study, changes in root hydraulic properties result in evolving root system HAs. As demonstrated by *Couvreur et al.* [2012], root system HA properties can be summarized in terms of their emergent macroscopic properties **SUF** and K_{rs}. Graphical representations of the **SUF** (vector defined in the root system domain, $[N \times 1]$ where N is the number of root segments) are shown at the scale of the soil element, or larger. For that, Standard Uptake Fractions that belong to the same soil element are simply summed up, which provides the Standard Sink Fraction distribution, **SSF** (-) $[M \times 1]$ where M is the number of soil elements. It is worth noting that the sum of the standard sink fractions is also 1, by definition.

The **SSF** corresponds to the weighting with which the plant senses each local SWP, and distributes its uptake in conditions of uniform SWP. In the two-dimensional representation of the "Default" **SSF** (Figure 5, left, for which standard sink fractions were summed up in the direction perpendicular to the maize row), the plant mostly senses SWP in the upper part of the profile, right below the row. Since this place is also the one to dry down the most during a drought event [*Hupet and Vanclooster*, 2002; *Beff et al.*, 2013], the plant

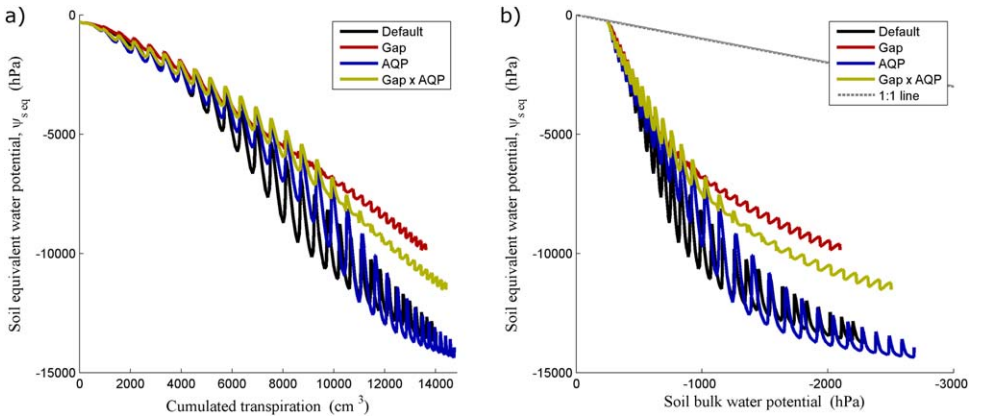

Figure 4. (a) Relation between cumulated transpiration and equivalent SWP during the simulated drought event. (b) Relation between bulk and equivalent SWPs during the simulated drought event.

generally tends to sense a $\psi_{s\ eq}$ far below the bulk SWP (i.e., SWP obtained from the average water content of the root zone, on the soil water retention curve), as shown in Figure 4b. When processes reducing the radial conductance between soil and root xylem with decreasing SWP (such as air gaps) occur, the root tends to be "hydraulically disconnected" from the drier area, and the **SSF** decreases in that area. Figure 5 (right) illustrates the consequent downward shift of **SSF** for the "Gap" HA, at the end of the drought scenario (day 31). This "avoidance" strategy [*Tardieu*, 2011] allows the plant not to sense the lowest SWPs and results in an increased and more stable $\psi_{s\ eq}$ (see "Gap" and "Gap x AQP" in Figure 4). Since ψ_{collar} equals $\psi_{s\ eq}$ when the plant does not transpire (see equation (2)), higher values of $\psi_{s\ eq}$ also explain the higher night water potentials for "Gap" and "Gap x AQP" in Figure 3b. Processes decreasing root radial conductance with soil drying could thus explain the experimental observation that overnight plant water potential tends to equilibrate itself with wetter zones of the soil, regardless of lowest values of SWPs in the profile [*Schmidhalter*, 1997; *Richter*, 1997].

Figure 6a shows that even though the "Gap" **SSF** progressively shifts downward with time, it slightly shifts back upward each night, due to the night-time redistribution of water by soil and roots, which partly refills upper soil layers and reestablishes contact between soil and roots. Except from a slight variation during the first week, the "AQP" **SSF** did not significantly fluctuate (see Figure 6b), probably due to the fact that, after 1 week, most of root segments already reached their maximum radial hydraulic conductance (located at −1000 hPa). The "AQP" **SSF** was also very similar to the "Default" **SSF**, suggesting that a proportional increase of all root radial conductances does not affect this emergent parameter.

As shown in Figure 7, the second emergent parameter, K_{rs}, is also dynamic during the simulated drought. A 24 h period dynamics (related to the period of T_{pot} variations), with increased conductance during the day can be noticed for the "AQP" HA during the first simulated days. Interestingly, the same plant conductance dynamics was empirically evidenced for maize [*Lopez et al*., 2003] and rice [*Sakurai-Ishikawa et al*., 2011] in hydroponic conditions, in which air gaps and/or hydrophobic layers do not form around roots. These authors showed AQP activity to increase with transpiration rate, but could as well have related it to root water potential, which is strongly correlated to transpiration rate. In opposition, processes reducing root radial conductivity with soil drying are shown to provoke a 24 h period dynamics of K_{rs} with peaks at night (see red and yellow lines in Figure 7).

As compared to $\psi_{s\ eq}$, each HA's relative K_{rs} follows the trend of local changes in relative root radial conductances (bright versus light colors in Figure 7), but smoothed downward. According to equation (2), each HA's K_{rs} defines the amplitude of day-night variation of ψ_{collar}, explaining, for instance, the narrow amplitude of "AQP" ψ_{collar} and increasing amplitude of "Gap x AQP" ψ_{collar} in Figure 3b.

These results illustrate the influence of local alterations of root radial conductances in drying soil on **SSF** and K_{rs}, which in turn affect plant water potential dynamics, respectively through their control on (i) the SWP sensed by the plant and (ii) plant water potential decrease due to transpiration ($-T_{act}/K_{rs}$, see equation (2)). This approach could help understand how different local sensitivities of radial conductances to soil

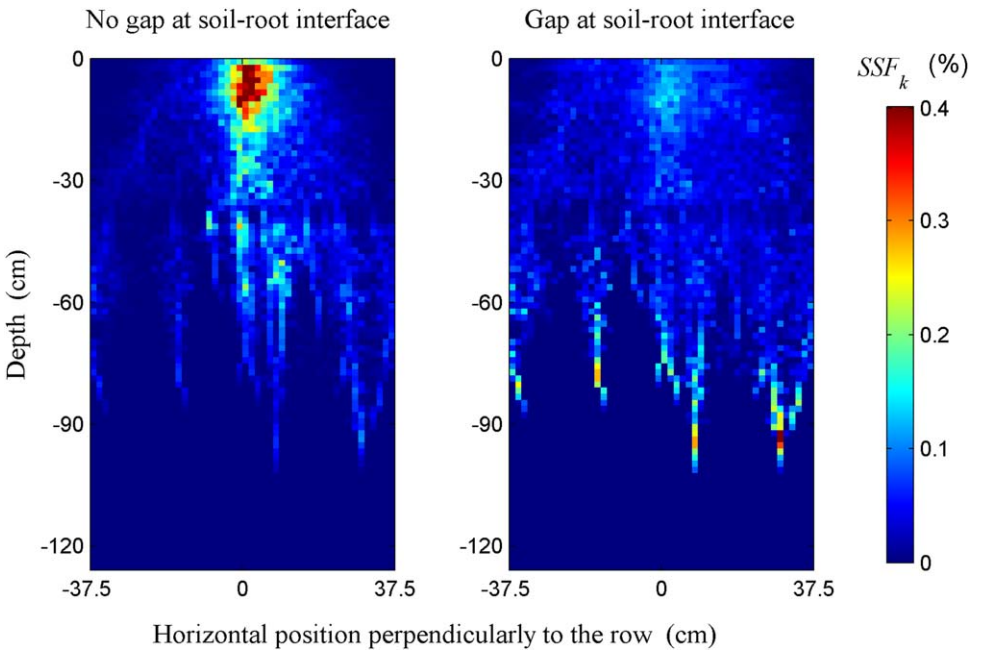

Figure 5. Two-dimensional (integrated in the direction of maize rows) standard sink fraction distributions of the (left) "Default" and (right) late "Gap" hydraulic architectures.

matric potential (i) translate into different plant-scale strategies for access to water, and (ii) define plant water potential, which is known to affect plant physiological processes such as organ growth [*Gardner and Nieman*, 1964; *Frensch and Hsiao*, 1994; *Shabala and Lew*, 2002; *Caldeira et al*., 2014].

4.3. Dynamics of the Water Flow Rate Available for Plant Transpiration

As discussed in section 2.2, K_{rs} determines the slope of the Q_{avail} limit to isohydric plants transpiration. Depending on the value of T_{pot}, the actual plant transpiration rate may be located on the Q_{avail} versus $\psi_{s\ eq}$ line (case of limiting flow rate available), or within the lower area delimited by the Q_{avail} versus $\psi_{s\ eq}$ line. This lower area contains all the possible values of plant transpiration rate for the plant HA, and is commonly called a "water use envelope" [*Sperry et al*., 1998]. The limits of this envelope are static for constant root system HAs, such as the "Default" one. However, as far as dynamic HAs are concerned, K_{rs} is dynamic and the slope of the Q_{avail} limit evolves with time.

In Figure 8a, points are displayed for which plant transpiration rate is limited by Q_{avail} during the simulations. As shown by the linear shape of "Default" and "AQP" water stress functions, pointing toward $\psi_{leaf\ lim}$, K_{rs} is not (or not significantly) dynamic during water stress periods for these HAs. The slopes of their respective Q_{avail} boundaries thus correspond to their K_{rs}, with notably a steeper limit for the "AQP" HA.

The Q_{avail} boundaries of "Gap" and "Gap x AQP" HAs are built by the succession of properties of their dynamic HAs. Even though the shape of the resulting boundary represented by the points in Figure 8a is remarkably linear, one should not mistake the value of its slope for K_{rs} (which is the slope of the line linking a point of the boundary to $\psi_{leaf\ lim}$, grey lines in Figure 8a). In other words, the equivalence between K_{rs} and the slope of the water stress function postulated in section 2.2 is not generally valid for dynamic plant HAs. In such conditions, a requisite to draw the water stress function from K_{rs} would be to know the trajectory of K_{rs} versus $\psi_{s\ eq}$ (see Figure 7). For instance, gray dots in Figure 7 mark a clear trend of couples $\left(K_{rs}; \psi_{s\ eq}\right)$ at the same time of the day during 10 consecutive days, which were used to draw the grey segments shaping the "Gap x AQP" Q_{avail} boundary in Figure 8a.

When building their root system, plants indirectly shape their Q_{avail} limit, whereas canopy development rather affects T_{pot}. As discussed by *Ewers et al*. [2000], the allocation of carbon between root and shoot systems has a major influence on the efficiency of resource acquisition. A plant whose transpiration rate (and by the same occasion photosynthesis) is limited by T_{pot} may increase the latter by allocating carbon to the

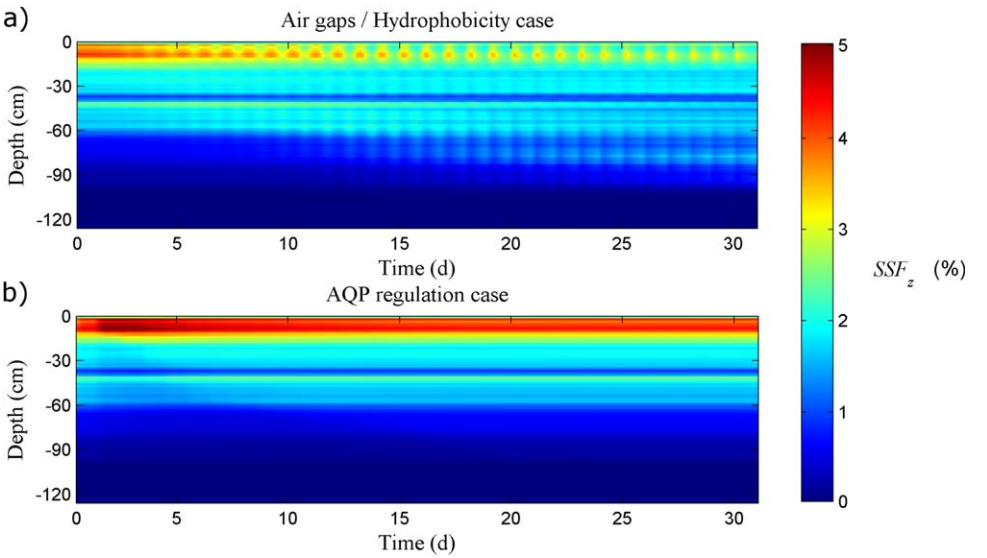

Figure 6. Time evolution of one-dimensional standard sink fraction distributions for (a) "Gap" and (b) "AQP" hydraulic architectures.

development of its canopy. Conversely, for an isohydric plant whose transpiration rate is limited by Q_{avail}, increasing the leaf area has no effect on the actual transpiration rate (even though T_{pot} is expected to increase), while an enhanced AQP activity or root production will increase K_{rs}, and consequently Q_{avail}. In conditions when water availability is the limiting factor to plant development, adjustments of the root to shoot ratio may thus be seen as a problem of shaping the area delimited by Q_{avail} and T_{pot} (see Figure 1a).

A final point discussed here is the relation between bulk SWP (water potential of the soil water retention curve corresponding to the average water content of the root zone) and $\psi_{s\ eq}$, which are expected to differ in case SWP is not uniform. As discussed in section 1.2, no simple function predicting water potential at soil-root interfaces exists for heterogeneous root distributions and transient uptake rates. In this study, the soil hydraulic limitation was simulated by solving Richards equation in 3-D, and resulted in values of $\psi_{s\ eq}$ significantly lower than the bulk SWP (see Figure 4b). Thus, even though the soil hydraulic resistance did not appear directly in our water stress functions, it actually influenced Q_{avail} through its effect on $\psi_{s\ eq}$.

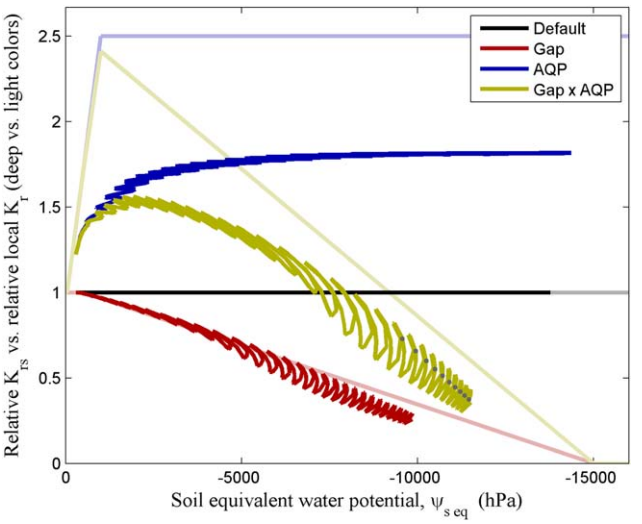

Figure 7. Relation between relative K_{rs} (relative to the Default hydraulic architecture) and the equivalent SWP ($\psi_{s\ eq}$) for each type of hydraulic architecture (bright colored lines), compared to the relation between local soil matric potential and root segment relative hydraulic conductivity (light-colored lines).

As shown in Figure 8b, using the bulk SWP as abscissa would result in a quite different and rather fuzzy stress function, also expected to change with T_{daily} (not shown). Using the bulk SWP as abscissa (Figure 8b), or $\psi_{s\ eq}$ with dynamic HAs (Figure 8a), yields water stress functions that seemingly have various endpoints higher than $\psi_{leaf\ lim}$, which could explain the difficulty to empirically identify the nature of water stress functions endpoints. In this study, all endpoints actually correspond to $\psi_{leaf\ lim}$, but realizing that water stress functions may be nonlinear and using the nonbulk measure of SWP ($\psi_{s\ eq}$) are necessary to reach that conclusion. The estimation of $\psi_{s\ eq}$ (for instance, by measuring

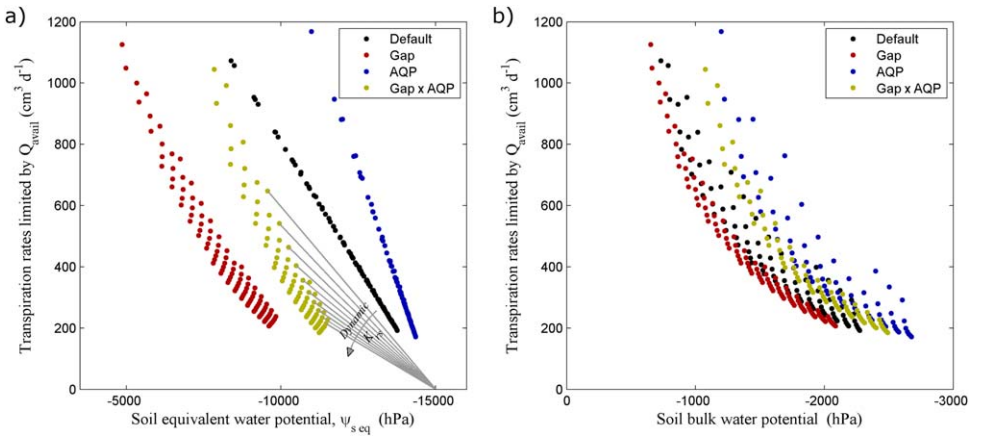

Figure 8. (a) Limiting water flow rates available from the drought scenario for each type of hydraulic architecture (10 observation points a day, only the limiting ones being displayed). (b) Relation between bulk SWP and limiting water flow rates available from the drought scenario for each type of hydraulic architecture (10 observation points a day, only the limiting ones being displayed).

plant predawn water potential) is thus a central point in the characterization of a mechanistic water stress function. Future prospects might focus on finding specific positions in the root zone where SWP is a good proxy of $\psi_{s\ eq}$ or calculate it using methods accounting for transient uptake rates and root system heterogeneity.

5. Conclusions and Outlook

The first objective of this study was to revisit the concept of soil water availability for plant transpiration, as impacted by root system hydraulic properties, in the light of physical concepts. Two limitations to soil water availability were put forward: (i) the stock of water consumable by the plant h_{avail} (L), as defined by *Veihmeyer and Hendrickson* [1927], and (ii) the rate at which this stock can be consumed, corresponding to the instantaneous "water flow rate available to plant leaves for transpiration" Q_{avail} ($L^3\ T^{-1}$). This limiting water flow rate was quantified as the product of the root system hydraulic conductance (K_{rs}) by the difference between the plant-sensed soil water potential ($\psi_{s\ eq}$) and the threshold leaf water potential ($\psi_{leaf\ lim}$), which triggers water stress in isohydric plants.

An analysis of similarities between the shape of empirical plant water stress functions and the Q_{avail} versus $\psi_{s\ eq}$ relation suggested that the permanent wilting point (PWP) and the slope of empirical stress functions could respectively correspond to the plant $\psi_{leaf\ lim}$ and the ratio of K_{rs} to the plant potential transpiration rate. When these properties would match, existing empirical water stress functions would deliver values of K_{rs} and $\psi_{leaf\ lim}$, while measuring K_{rs} and $\psi_{leaf\ lim}$ would represent a convenient way to shape our future empirical plant water stress functions. However, it was demonstrated that this equality might not hold in case the hydraulic conductance between soil-root interface and root xylem would depend on soil matric potential.

The second objective was to understand how plant water availability may be affected by the local dynamism of hydraulic conductances between soil and root xylem, possibly resulting from processes such as the formation of air gaps at soil-root interfaces and the regulation of aquaporins activity. Soil-plant hydrodynamics was simulated in 3-D for a maize crop whose root radial conductances would either locally decrease ("Gap" scenario), or increase ("AQP" scenario), or combine both trends ("Gap x AQP" scenario), with decreasing soil matric potential. The resulting dynamic hydraulic architectures (HAs) had exactly the same root system architecture, and the same initial h_{avail}, but showed radically different responses to water deficit, which could be interpreted as contrasting strategic behaviors adapted to different types of environmental conditions. The "Gap" scenario was characterized by early water stress, but also by a better recovery of plant water potential at night. The latter particularity was due to the shift of the standard uptake fraction distribution (**SSF**) toward wet zones, which could explain the experimental observation that plant water potential tends to equilibrate with wetter zones of the soil overnight. In the "AQP" scenario, the increased K_{rs} enhanced root hydraulic redistribution and temporarily increased plant access to water, but resulted in

lower Q_{avail} at long term. Eventually, as compared to a "Default" HA with constant hydraulic properties, the "Gap x AQP" HA could keep both of its cumulative transpiration rate and average water potential at soil-root interfaces ($\psi_{s\ eq}$) higher, combining the advantages of "Gap" and "AQP" HAs.

It must be noted that soil water availability for plant transpiration was also limited by soil hydraulic resistivity, which was accounted for in the simulations by explicitly solving the Richards equation with a high spatial resolution. The additional impact of this soil resistance resulted in values of $\psi_{s\ eq}$ significantly lower than the bulk SWP.

In this study, the modeling platform R-SWMS proved to be a convenient tool to investigate and quantify the result of interactions between complex and nonlinear processes involved in soil-plant hydrodynamics. In the future, such insight might help crop breeders selecting root phenotypes improving soil water availability in water-limited environments as in *Leitner et al.* [2014]. But before that, several other relations might need to be considered in a more detailed model, including (i) the genotype by environment impact on plant phenotype, (ii) stomatal adjustments of water "demand" in response to leaf environment, (iii) plant growth and carbon allocation, and (iv) a better understanding of processes affecting plant hydraulic properties, such as AQP activity regulation, the formation of air gaps at soil-root interfaces and xylem cavitation. Models concentrating on other complex mechanisms, such as hydraulic and hormonal regulation of stomata [*Tardieu and Simonneau*, 1998; *Christmann et al*., 2007; *Franks et al*., 2007; *McAdam and Brodribb*, 2014; *Huber et al*., 2014], genome by environment interactions [*Hammer et al*., 2006], and plant transpiration versus growth for a single plant [*Dunbabin et al*., 2002; *Drouet and Pages*, 2003; *Fourcaud et al*., 2008; *Caldeira et al*., 2014] or for a community of plants [*Cramer et al*., 2001; *Bonan et al*., 2003; *Sterck and Schieving*, 2011], have been proposed in the literature. This study did not integrate the latter processes but explicitly investigated the relation between root segment-scale hydraulics and whole root system hydraulics. These relations could be coupled with large-scale models needing estimations of leaf water potential and soil water availability but also in more detailed models that consider shoot hydraulics [*Janott et al*., 2011] or regulation of relative transpiration by root zone produced chemical signals [*Huber et al*., 2014]. This coupling will allow investigating differences in the relation between soil water status and transpiration rates between plants with different control mechanisms (hydraulic versus hormonal signaling, isohydric versus anisohydric plants) and will be useful to improve the relations between leaf-scale stomatal conductance and the effective stomatal conductance at the plant scale. Finally, the coupling of models that improve the prediction of water supply to a plant with models that simulate water demand and growth is essential for predicting feedbacks between supply, demand, and growth under water limited conditions.

Acknowledgments

The simulation data displayed in section 4 of this research article were obtained by running the program R-SWMS [*Javaux et al*., 2008] at Jülich Supercomputing Center. The complete data set is available on demand to V. Couvreur, M. Javaux, and J. Vanderborght. The authors would like to thank Andrea Carminati, Brent Ewers, Jan Hopmans, Walid Sadok, Sjoerd van der Zee, and two anonymous referees for their constructive comments, which helped improving the quality of the manuscript. During the preparation of this manuscript, V.C. was supported by the "Fonds National de la Recherche Scientifique" of Belgium (FNRS) as Research Fellow, by the "Belgian American Educational Foundation" (BAEF) as UCLouvain Fellow, by "Wallonie-Bruxelles International" (WBI) with a WBI.WORLD excellence grant, and by the "Fonds Spéciaux de Recherche" of the Université catholique de Louvain.

References

Allen, R. G., L. S. Pereira, D. Raes, and M. Smith (1998), Crop evapotranspiration—Guidelines for computing crop water requirements, *FAO Irrig. Drain. Pap. 56*, U. N. Food and Agric. Organ., Rome.

Barrowclough, D. E., C. A. Peterson, and E. Steudle (2000), Radial hydraulic conductivity along developing onion roots, *J. Exp. Bot.*, *51*, 547–557, doi:10.1093/jexbot/51.344.547.

Beff, L., T. Günther, B. Vandoorne, V. Couvreur, and M. Javaux (2013), Three-dimensional monitoring of soil water content in a maize field using Electrical Resistivity Tomography, *Hydrol. Earth Syst. Sci.*, *17*, 595–609.

Bonan, G. B., S. Levis, S. Sitch, M. Vertenstein, and K. W. Oleson (2003), A dynamic global vegetation model for use with climate models: Concepts and description of simulated vegetation dynamics, *Global Change Biol.*, *9*, 1543–1566, doi:10.1046/j.1365-2486.2003.00681.x.

Brooksbank, K., D. A. White, E. J. Veneklaas, and J. L. Carter (2011), Hydraulic redistribution in Eucalyptus kochii subsp. borealis with variable access to fresh groundwater, *Trees Struct. Funct.*, *25*, 735–744.

Caldeira, C. F., M. Bosio, B. Parent, L. Jeanguenin, F. Chaumont, and F. Tardieu (2014), A hydraulic model is compatible with rapid changes in leaf elongation under fluctuating evaporative demand and soil water status, *Plant Physiol.*, *164*, 1718–1730.

Caldwell, M. M., and J. H. Richards (1989), Hydraulic lift: Water efflux from upper roots improves effectiveness of water uptake by deep roots, *Oecologia*, *79*, 1–5.

Carminati, A., and D. Vetterlein (2013), Plasticity of rhizosphere hydraulic properties as a key for efficient utilization of scarce resources, *Ann. Bot. London*, *112*, 277–290.

Carminati, A., D. Vetterlein, U. Weller, H. J. Vogel, and S. E. Oswald (2009), When roots lose contact, *Vadose Zone J.*, *8*, 805–809, doi:10.2136/vzj2008.0147.

Carsel, R. F., and R. S. Parrish (1988), Developping joint probability-distributions of soil-water retention characteristics, *Water Resour. Res.*, *24*, 195–200.

Chaumont, F., M. Moshelion, and M. J. Daniels (2005), Regulation of plant aquaporin activity, *Biol. Cell*, *97*, 749–764, doi:10.1042/BC20040133.

Chenu, K., S. C. Chapman, G. L. Hammer, G. McLean, H. B. H. Salah, and F. Tardieu (2008), Short-term responses of leaf growth rate to water deficit scale up to whole-plant and crop levels: An integrated modelling approach in maize, *Plant Cell Environ.*, *31*, 378–391, doi:10.1111/j.1365-3040.2007.01772.x.

Christmann, A., E. W. Weiler, E. Steudle, and E. Grill (2007), A hydraulic signal in root-to-shoot signalling of water shortage, *Plant J.*, *52*, 167–174.

Cochard, H., L. Coll, X. Le Roux, and T. Ameglio (2002), Unraveling the effects of plant hydraulics on stomatal closure during water stress in walnut, *Plant Physiol.*, *128*, 282–290, doi:10.1104/pp.010400.

Couvreur, V., J. Vanderborght, and M. Javaux (2012), A simple three-dimensional macroscopic root water uptake model based on the hydraulic architecture approach, *Hydrol. Earth Syst. Sci.*, *16*, 2957–2971.
Couvreur, V., J. Vanderborght, L. Beff, and M. Javaux (2014), Horizontal soil water potential heterogeneity: Simplifying approaches for crop water dynamics models, *Hydrol. Earth Syst. Sci.*, *18*, 1723–1743.
Cramer, W., et al. (2001), Global response of terrestrial ecosystem structure and function to CO_2 and climate change: Results from six dynamic global vegetation models, *Global Change Biol.*, *7*, 357–373, doi:10.1046/j.1365-2486.2001.00383.x.
Damour, G., T. Simonneau, H. Cochard, and L. Urban (2010), An overview of models of stomatal conductance at the leaf level, *Plant Cell Environ.*, *33*, 1419–1438, doi:10.1111/j.1365-3040.2010.02181.x.
Dawson, T. E. (1996), Determining water use by trees and forests from isotopic, energy balance and transpiration analyses: The roles of tree size and hydraulic lift, *Tree Physiol.*, *16*, 263–272.
De Jong Van Lier, Q., K. Metselaar, and J. C. Van Dam (2006), Root water extraction and limiting soil hydraulic conditions estimated by numerical simulation, *Vadose Zone J.*, *5*, 1264–1277.
Dodd, I. C., G. Egea, C. W. Watts, and W. R. Whalley (2010), Root water potential integrates discrete soil physical properties to influence ABA signalling during partial rootzone drying, *J. Exp. Bot.*, *61*, 3543–3551, doi:10.1093/jxb/erq195.
Domec, J. C., and M. L. Pruyn (2008), Bole girdling affects metabolic properties and root, trunk and branch hydraulics of young ponderosa pine trees, *Tree Physiol.*, *28*, 1493–1504.
Doussan, C., L. Pages, and G. Vercambre (1998a), Modelling of the hydraulic architecture of root systems: An integrated approach to water absorption—Model description, *Ann. Bot. London*, *81*, 213–223.
Doussan, C., G. Vercambre, and L. Pages (1998b), Modelling of the hydraulic architecture of root systems: An integrated approach to water absorption—Distribution of axial and radial conductances in maize, *Ann. Bot. London*, *81*, 225–232.
Doussan, C., A. Pierret, E. Garrigues, and L. Pages (2006), Water uptake by plant roots: II—Modelling of water transfer in the soil root-system with explicit account of flow within the root system—Comparison with experiments, *Plant Soil*, *283*, 99–117.
Drouet, J. L., and L. Pages (2003), GRAAL: A model of GRowth, Architecture and carbon ALlocation during the vegetative phase of the whole maize plant—Model description and parameterisation, *Ecol. Model.*, *165*, 147–173.
Dunbabin, V. M., A. J. Diggle, Z. Rengel, and R. van Hugten (2002), Modelling the interactions between water and nutrient uptake and root growth, *Plant Soil*, *239*, 19–38.
Ewers, B. E., R. Oren, and J. S. Sperry (2000), Influence of nutrient versus water supply on hydraulic architecture and water balance in Pinus taeda, *Plant Cell Environ.*, *23*, 1055–1066, doi:10.1046/j.1365-3040.2000.00625.x.
Feddes, R. A., P. Kowalik, K. Kolinska-Malinka, and H. Zaradny (1976), Simulation of field water uptake by plants using a soil water dependent root extraction function, *J. Hydrol.*, *31*, 13–26.
Feddes, R. A., P. J. Kowalik, and H. Zaradny (1978), *Simulation of Field Water Use and Crop Yield*, 189 pp., Pudoc, Simul. Monogr., Wageningen, Netherlands.
Fisher, R. A., M. Williams, R. L. Do Vale, A. L. Da Costa, and P. Meir (2006), Evidence from Amazonian forests is consistent with isohydric control of leaf water potential, *Plant Cell Environ.*, *29*, 151–165, doi:10.1111/j.1365-3040.2005.01407.x.
Fourcaud, T., X. Zhang, A. Stokes, H. Lambers, and C. Korner (2008), Plant growth modelling and applications: The increasing importance of plant architecture in growth models, *Ann. Bot. London*, *101*, 1053–1063.
Franks, P. J., P. L. Drake, and R. H. Froend (2007), Anisohydric but isohydrodynamic: Seasonally constant plant water potential gradient explained by a stomatal control mechanism incorporating variable plant hydraulic conductance, *Plant Cell Environ.*, *30*, 19–30, doi:10.1111/j.1365-3040.01600.x.
Frensch, J., and T. C. Hsiao (1994), Transient responses of cell turgor and growth of maize roots as affected by changes in water potential, *Plant Physiol.*, *104*, 247–254.
Frensch, J., and E. Steudle (1989), Axial and radial hydraulic resistance to roots of maize (Zea-mays-L), *Plant Physiol.*, *91*, 719–726.
Gardner, W. R. (1965), Dynamic aspects of soil-water availability to plants, *Ann. Rev. Plant Physiol.*, *16*, 323–342, doi:10.1146/annurev.pp.16.060165.001543.
Gardner, W. R., and C. F. Ehlig (1963), The influence of soil water on transpiration by plants, *J. Geophys. Res.*, *68*, 5719–5724.
Gardner, W. R., and R. H. Nieman (1964), Lower limit of water availability to plants, *Science*, *143*, 1460–1462, doi:10.1126/science.143.3613.1460.
Girardin, P. (1970), *Ecophysiologie du maïs*, edited by AGPM, Arvalis, Montardon, France.
Gracheva, I., A. Karimov, H. Turral, and F. Miryusupov (2009), An assessment of the potential and impacts of winter water banking in the Sokh aquifer, Central Asia, *Hydrogeol. J.*, *17*, 1471–1482, doi:10.1007/s10040-009-0444-0.
Hammer, G., M. Cooper, F. Tardieu, S. Welch, B. Walsh, F. van Eeuwijk, S. Chapman, and D. Podlich (2006), Models for navigating biological complexity in breeding improved crop plants, *Trends Plant Sci.*, *11*, 587–593, doi:10.1016/j.tplants.2006.10.006.
Hose, E., E. Steudle, and W. Hartung (2000), Abscisic acid and hydraulic conductivity of maize roots: A study using cell- and root-pressure probes, *Planta*, *211*, 874–882, doi:10.1007/s004250000412.
Huber, K., J. Vanderborght, M. Javaux, N. Schröder, I. Dodd, and H. Vereecken (2014), Modelling the impact of heterogeneous rootzone water distribution on the regulation of transpiration by hormone transport and/or hydraulic pressures, *Plant Soil*, *384*, 1–2, doi:10.1007/s11104-014-2188-4.
Hupet, F., and M. Vanclooster (2002), Intraseasonal dynamics of soil moisture variability within a small agricultural maize cropped field, *J. Hydrol.*, *261*, 86–101.
Janott, M., S. Gayler, A. Gessler, M. Javaux, C. Klier, and E. Priesack (2011), A one-dimensional model of water flow in soil-plant systems based on plant architecture, *Plant Soil*, *341*, 233–256.
Jarvis, N. J. (1989), A simple empirical model of root water uptake, *J. Hydrol.*, *107*, 57–72.
Javaux, M., T. Schroder, J. Vanderborght, and H. Vereecken (2008), Use of a three-dimensional detailed modeling approach for predicting root water uptake, *Vadose Zone J.*, *7*, 1079–1088.
Javaux, M., V. Couvreur, J. Vanderborght, and H. Vereecken (2013), Root water uptake: From 3D biophysical processes to macroscopic modeling approaches, *Vadose Zone J.*, *12*, 1–16, doi:10.2136/vzj2013.02.0042.
Jennings, G. D. (1996), *Hydraulic Ram Pumps*, N. C. Coop. Ext. Serv., N. C.
Khodarahmpour, Z., and J. Hamidi (2012), Study of yield and yield components of corn (Zea mays L.) inbred lines to drought stress, *Afr. J. Biotechnol.*, *11*, 3099–3105.
Kholova, J., C. T. Hash, A. Kakkera, M. Kocova, and V. Vadez (2010), Constitutive water-conserving mechanisms are correlated with the terminal drought tolerance of pearl millet Pennisetum glaucum (L.) R. Br., *J. Exp. Bot.*, *61*, 369–377, doi:10.1093/jxb/erp314.
Kolb, K. J., and J. S. Sperry (1999), Transport constraints on water use by the Great Basin shrub, Artemisia tridentata, *Plant Cell Environ.*, *22*, 925–935.

Leitner, D., F. Meunier, G. Bodner, M. Javaux, and A. Schnepf (2014), Impact of contrasted maize root traits at flowering on water stress tolerance—A simulation study, *Field Crops Res.*, *165*, 125–137.
Lobet, G., V. Couvreur, F. Meunier, M. Javaux, and X. Draye (2014), Plant water uptake in drying soils, *Plant Physiol.*, *164*, 1619–1627, doi:10.1104/pp.113.233486.
Loewenstein, N. J., and S. G. Pallardy (1998), Drought tolerance, xylem sap abscisic acid and stomatal conductance during soil drying: A comparison of canopy trees of three temperate deciduous angiosperms, *Tree Physiol.*, *18*, 431–439.
Lopez, F., A. Bousser, I. Sissoeff, M. Gaspar, B. Lachaise, J. Hoarau, and A. Mahe (2003), Diurnal regulation of water transport and aquaporin gene expression in maize roots: Contribution of PIP2 proteins, *Plant Cell Physiol.*, *44*, 1384–1395, doi:10.1093/pcp/pcg168.
Maurel, C., and M. J. Chrispeels (2001), Aquaporins. A molecular entry into plant water relations, *Plant Physiol.*, *125*, 135–138, doi:10.1104/pp.125.1.135.
Maurel, C., J. Reizer, J. I. Schroeder, and M. J. Chrispeels (1993), The vacuolar membrane-protein gamma-tip creates water specific channels in xenopus-oocytes, *Embo J.*, *12*, 2241–2247.
McAdam, S. A. M., and T. J. Brodribb (2014), Separating active and passive influences on stomatal control of transpiration, *Plant Physiol.*, *164*, 1578–1586, doi:10.1104/pp.113.231944.
McDowell, N., et al. (2008), Mechanisms of plant survival and mortality during drought: why do some plants survive while others succumb to drought?, *New Phytol.*, *178*, 719–739, doi:10.1111/j.1469-8137.2008.02436.x.
McElrone, A. J., J. Bichler, W. T. Pockman, R. N. Addington, C. R. Linder, and R. B. Jackson (2007), Aquaporin-mediated changes in hydraulic conductivity of deep tree roots accessed via caves, *Plant Cell Environ.*, *30*, 1411–1421, doi:10.1111/j.1365-3040.2007.01714.x.
Novak, V., and J. Havrila (2006), Method to estimate the critical soil water content of limited availability for plants, *Biologia*, *61*, S289–S293, doi:10.2478/s11756-006-0175-9.
Pages, L., G. Vercambre, J. L. Drouet, F. Lecompte, C. Collet, and J. Le Bot (2004), Root Typ: A generic model to depict and analyse the root system architecture, *Plant Soil*, *258*, 103–119.
Richter, H. (1997), Water relations of plants in the field: Some comments on the measurement of selected parameters, *J. Exp. Bot.*, *48*, 1–7, doi:10.1093/jxb/48.1.1.
Sakurai-Ishikawa, J., M. Murai-Hatano, H. Hayashi, A. Ahamed, K. Fukushi, T. Matsumoto, and Y. Kitagawa (2011), Transpiration from shoots triggers diurnal changes in root aquaporin expression, *Plant Cell Environ.*, *34*, 1150–1163, doi:10.1111/j.1365-3040.2011.02313.x.
Schmidhalter, U. (1997), The gradient between pre-dawn rhizoplane and bulk soil matric potentials, and its relation to the pre-dawn root and leaf water potentials of four species, *Plant Cell Environ.*, *20*, 953–960, doi:10.1046/j.1365-3040.1997.d01-136.x.
Schoppach, R., and W. Sadok (2012), Differential sensitivities of transpiration to evaporative demand and soil water deficit among wheat elite cultivars indicate different strategies for drought tolerance, *Environ. Exp. Bot.*, *84*, 1–10.
Schröder, N., N. Lazarovitch, J. Vanderborght, H. Vereecken, and M. Javaux (2014), Linking transpiration reduction to rhizosphere salinity using a 3D coupled soil-plant model, *Plant Soil*, *377*, 277–293, doi:10.1007/s11104-013-1990-8.
Schroeder, T., L. Tang, M. Javaux, J. Vanderborght, B. Körfgen, and H. Vereecken (2009), A grid refinement approach for a three-dimensional soil-root water transfer model, *Water Resour. Res.*, *45*, W10412, doi:10.1029/2009WR007873.
Sene, K. J., T. J. Marsh, and A. Hachache (1999), An assessment of the difficulties in quantifying the surface water resources of Lebanon, *Hydrol. Sci. J.*, *44*, 79–96, doi:10.1080/02626669909492204.
Shabala, S. N., and R. R. Lew (2002), Turgor regulation in osmotically stressed Arabidopsis epidermal root cells. Direct support for the role of inorganic ion uptake as revealed by concurrent flux and cell turgor measurements, *Plant Physiol.*, *129*, 290–299, doi:10.1104/pp.020005.
Shackel, K. (2011), A plant-based approach to deficit irrigation in trees and vines, *Hortscience*, *46*, 173–177.
Sinclair, T. R. (2005), Theoretical analysis of soil and plant traits influencing daily plant water flux on drying soils, *Agron. J.*, *97*, 1148–1152, doi:10.2134/agronj2004.0286.
Siqueira, M., G. Katul, and A. Porporato (2008), Onset of water stress, hysteresis in plant conductance, and hydraulic lift: Scaling soil water dynamics from millimeters to meters, *Water Resour. Res.*, *44*, W01432, doi:10.1029/2007WR006094.
Somma, F., J. W. Hopmans, and V. Clausnitzer (1998), Transient three-dimensional modeling of soil water and solute transport with simultaneous root growth, root water and nutrient uptake, *Plant Soil*, *202*, 281–293, doi:10.1023/A:1004378602378.
Sperry, J. S., F. R. Adler, G. S. Campbell, and J. P. Comstock (1998), Limitation of plant water use by rhizosphere and xylem conductance: Results from a model, *Plant Cell Environ.*, *21*, 347–359, doi:10.1046/j.1365-3040.1998.00287.x.
Steduto, P., T. C. Hsiao, D. Raes, and E. Fereres (2009), AquaCrop—The FAO crop nodel to simulate yield response to water: I. Concepts and underlying principles, *Agron. J.*, *101*, 426–437, doi:10.2134/agronj2008.0139s.
Sterck, F., and F. Schieving (2011), Modelling functional trait acclimation for trees of different height in a forest light gradient: Emergent patterns driven by carbon gain maximization, *Tree Physiol.*, *31*, 1024–1037, doi:10.1093/treephys/tpr065.
Tanner, C. B. (1967), Measurement of evapotranspiration, *Agronomy*, *11*, 534–574.
Tardieu, F. (1988), Analysis of the spatial variability of maize root density. 2. Distances between roots, *Plant Soil*, *107*, 267–272.
Tardieu, F. (2011), Any trait or trait-related allele can confer drought tolerance: Just design the right drought scenario, *J. Exp. Bot.*, *63*, 25–31, doi:10.1093/jxb/err269.
Tardieu, F., and W. J. Davies (1992), Stomatal response to abscisic-acid is a function of current plant water status, *Plant Physiol.*, *98*, 540–545, doi:10.1104/pp.98.2.540.
Tardieu, F., and S. Pellerin (1990), Trajectory of the nodal roots of maize in fields with low mechanical constraints, *Plant Soil*, *124*, 39–45.
Tardieu, F., and T. Simonneau (1998), Variability among species of stomatal control under fluctuating soil water status and evaporative demand: Modelling isohydric and anisohydric behaviours, *J. Exp. Bot.*, *49*, 419–432, doi:10.1093/jexbot/49.suppl_1.419.
Tuzet, A., A. Perrier, and R. Leuning (2003), A coupled model of stomatal conductance, photosynthesis and transpiration, *Plant Cell Environ.*, *26*, 1097–1116.
Tyerman, S. D., C. M. Niemietz, and H. Bramley (2002), Plant aquaporins: Multifunctional water and solute channels with expanding roles, *Plant Cell Environ.*, *25*, 173–194, doi:10.1046/j.0016-8025.2001.00791.x.
Van Genuchten, M. T. (1980), A closed form equation for predicting the hydraulic conductivity of unsaturated soils, *Soil Sci. Soc. Am. J.*, *44*, 892–898.
Veihmeyer, F. J., and A. H. Hendrickson (1927), Soil-moisture conditions in relation to plant growth, *Plant Physiol.*, *2*, 71–82, doi:10.1104/pp.2.1.71.
Wesseling, J. G. (1991), Meerjarige simulatie van grondwaterstroming voor verschillende bodemprofielen, grondwatertrappen en gewassen met het model SWATRE, *Rapp. 152*, DLO-Staring Centrum, Wageningen, Netherlands.